Plant Communications
Research Article

CellPress
Partner Journal

SIZ1-Mediated SUMO Modification of SEUSS Regulates Photomorphogenesis in *Arabidopsis*

Xinyu Zhang[1,2,4], Junling Huai[1], Shuangrong Liu[1,2], Jing Bo Jin[2,3] and Rongcheng Lin[1,2,*]

[1]Key Laboratory of Photobiology, Institute of Botany, Chinese Academy of Sciences, Beijing 100093, China

[2]University of Chinese Academy of Sciences, Beijing 100049, China

[3]Key Laboratory of Plant Molecular Physiology, Institute of Botany, Chinese Academy of Sciences, Beijing 100093, China

[4]Present address: Department of Plant Sciences, University of Oxford, South Parks Road, Oxford OX1 3RB, UK

***Correspondence: Rongcheng Lin (rclin@ibcas.ac.cn)**

https://doi.org/10.1016/j.xplc.2020.100080

ABSTRACT

Small ubiquitin-like modifier (SUMO) post-translational modification (SUMOylation) plays essential roles in regulating various biological processes; however, its function and regulation in the plant light signaling pathway are largely unknown. SEUSS (SEU) is a transcriptional co-regulator that integrates light and temperature signaling pathways, thereby regulating plant growth and development in *Arabidopsis thaliana*. Here, we show that SEU is a substrate of SUMO1, and that substitution of four conserved lysine residues disrupts the SUMOylation of SEU, impairs its function in photo- and thermomorphogenesis, and enhances its interaction with PHYTOCHROME-INTERACTING FACTOR 4 transcription factors. Furthermore, the SUMO E3 ligase SIZ1 interacts with SEU and regulates its SUMOylation. Moreover, SEU directly interacts with phytochrome B photoreceptors, and the SUMOylation and stability of SEU are activated by light. Our study reveals a novel post-translational modification mechanism of SEU in which light regulates plant growth and development through SUMOylation-mediated protein stability.

Keywords: light signaling, phytochrome, PIF4, SUMOylation

Zhang X., Huai J., Liu S., Jin J.B., and Lin R. (2020). SIZ1-Mediated SUMO Modification of SEUSS Regulates Photomorphogenesis in *Arabidopsis*. Plant Comm. **1**, 100080.

INTRODUCTION

As a major environmental signal, light affects the growth and development of plants throughout their life cycle. Photomorphogenesis, the light-mediated development of plants, has been extensively studied in the model plant species *Arabidopsis thaliana*. Seedlings grown in darkness display elongated hypocotyls and closed cotyledons without chloroplast differentiation. Light triggers photomorphogenic responses, characterized by the inhibition of hypocotyl growth and the expansion of cotyledons that subsequently form functional chloroplasts. Multiple photoreceptors, including phytochromes (phy), cryptochromes, and UVR8, perceive light signals and activate various signaling pathways that ultimately control photomorphogenesis (Gommers and Monte, 2018). Numerous downstream components in the light signaling pathway have been identified, and their activities are regulated at transcriptional and post-translational levels (Hoecker, 2005; Jiao et al., 2007).

Transcription factors and their co-regulators play fundamental roles in controlling gene expression during photomorphogenesis (Jiao et al., 2007). PHYTOCHROME-INTERACTING FACTORS (PIFs) are a group of transcription factors possessing a conserved basic helix-loop-helix domain that negatively and redundantly regulates photomorphogenesis (Leivar and Monte, 2014). Plants with simultaneous loss of *PIF1*, *PIF3*, *PIF4*, and *PIF5* exhibit a photomorphogenic phenotype in darkness, similar to that of the *constitutive photomorphogenic1* (*cop1*) mutant (Leivar et al., 2008; Shin et al., 2009). When plants are irradiated with red light, the bioactive Pfr form of phy translocates from the cytoplasm to the nucleus, where it interacts with PIF proteins and degrades them through the 26S proteasome pathway (Ni et al., 2014). Genome-wide transcriptomic analyses reveal that PIF proteins regulate a large number of genes either directly or indirectly (Leivar et al., 2009; Shin et al., 2009; Pfeiffer et al., 2014).

A forward genetic study led to the identification of SEUSS (SEU) as a negative transcriptional regulator of photomorphogenesis (Huai et al., 2018). SEU is a homolog of the family of LDB proteins, which couple transcription factors to form high-order activation complexes in animals (Jurata and Gill, 1997). SEU

Published by the Plant Communications Shanghai Editorial Office in association with Cell Press, an imprint of Elsevier Inc., on behalf of CSPB and IPPE, CAS.

associates with the promoters of downstream cell elongation-related genes and regulates their expression by directly interacting with PIF4. The SEU–PIF4 interaction also positively regulates thermomorphogenesis (Huai et al., 2018). The short-hypocotyl phenotype of the *seu* knockout suggests that SEU might regulate plant growth and development at the adult stage independently of PIF4. Indeed, SEU functions as a transcriptional co-repressor with LEUING to regulate multiple developmental processes (Franks et al., 2002; Sridhar et al., 2006; Grigorova et al., 2011; Gong et al., 2016). Although the expression of SEU at the mRNA level is not drastically affected by light (Huai et al., 2018), its regulation at the protein level remains elusive.

The stability, activity, interaction, and/or localization of a protein are often regulated by post-translational modifications. SUMOylation is a key post-translational modification that covalently attaches small ubiquitin-like modifiers (SUMO) to certain lysine residues of target proteins (Johnson, 2004; Elrouby and Coupland, 2010). The SUMOylation machinery consists of the SUMO-activating enzyme, the SUMO-conjugating enzyme, and the SUMO E3 and E4 ligases. In *Arabidopsis*, SCE1 is a SUMO-conjugating enzyme, whereas SIZ1 is a SUMO E3 ligase (Park et al., 2011; Zhang et al., 2017b; Cai et al., 2017). SIZ1 mediates the conjugation of SUMO1/2 to its target proteins (Miura et al., 2005). Growing evidence indicates that SUMOylation plays critical regulatory roles in various plant developmental processes and responses to environmental cues (Miura et al., 2007, 2009; Jin et al., 2008; Park et al., 2011; Zheng et al., 2012; Conti et al., 2014; Kim et al., 2015; Crozet et al., 2016; Lin et al., 2016; Orosa et al., 2018). Two previous studies have shown that SUMOylation is involved in regulating light response. Phytochrome B (phyB) is subject to SUMOylation, which represses red light signaling partly by inhibiting the phyB–PIF5 interaction (Sadanandom et al., 2015). SIZ1 targets COP1 for SUMO modification and promotes COP1 activity, thereby negatively regulating photomorphogenesis, and COP1 in turn mediates the ubiquitination and degradation of SIZ1 (Lin et al., 2016). However, it is unknown whether and how the other components of the light signaling pathway are modified by SUMOylation.

In this study, we show that SEU undergoes SUMOylation at four conserved lysine sites and that substitution of these residues results in altered SEU activity and function. SIZ1 mediates the SUMOylation of SEU through direct interaction. In addition, phyB physically interacts with SEU and regulates its light-mediated protein stability. This study demonstrates that SEU SUMOylation plays essential roles in controlling plant growth and development in response to light.

RESULTS

SEU Is a Substrate of SUMO1

SUMO peptides are covalently linked to a SUMO consensus motif (ΨKxE/D; Ψ, large hydrophobic residue; K, acceptor lysine; x, any amino acid; E/D, glutamate or aspartate) in target proteins (Seeler and Dejean, 2003). To investigate the possible SUMO modification of SEU, we performed SUMOylation site prediction using three independent computational programs and found that SEU possesses four putative SUMOylation sites, K170, K200, K216, and K392, which are conserved in various plant species (Figure 1A, Supplemental Figure 1). This result suggests that SEU is likely a SUMO substrate.

To test this possibility, we performed transient *in vitro* and *in vivo* SUMOylation experiments. Firstly, we transiently coexpressed SEU-3HA with FLAG-SUMO1^{GG} (wild type) or FLAG-SUMO1^{AA} (a conjugation-deficient mutant) in *Arabidopsis* protoplasts. We then immunoprecipitated SEU-3HA with an anti-HA antibody and detected the immunoprecipitated proteins with an anti-FLAG antibody. Higher-molecular-weight SUMOylated SEU-3HA bands (SUMO1-SEU) were detected when SEU-3HA was coexpressed with FLAG-SUMO1^{GG}, but not with FLAG-SUMO1^{AA} (Figure 1B). Secondly, we performed a transient SUMOylation assay in *Nicotiana benthamiana* leaves and obtained similar results (Figure 1C). Thirdly, we generated *SEUp:SEU-GFP* transgenic plants, where *SEU* was fused with GFP and driven by its native promoter in the *seu-6* background. We extracted proteins from *seu-6* and *seu-6/SEUp:SEU-GFP* plants and immunoprecipitated them with anti-SEU and anti-SUMO1 antibodies. The anti-SUMO1 antibody detected higher-molecular-weight bands of SEU-GFP in *seu-6/SEUp:SEU-GFP*, but not *seu-6* plants (Figure 1D). There were two higher-molecular-weight bands whose exact weights differed from those in *Arabidopsis* protoplast and *N. benthamiana* assays, indicating that SEU may be multi- or poly-SUMOylated at one or more conjugating sites in different plants. Fourthly, we incubated affinity-purified recombinant proteins MBP-SEU-FLAG (substrate), SUMO E1 (His-SAE1b and His-SAE2), and SUMO E2 (His-SCE1) with His-SUMO1^{GG} or His-SUMO1^{AA} in the presence or absence of SUMO E3 ligase (MBP-SIZ1-Myc). Anti-FLAG and anti-SUMO1 antibodies detected slowly migrating bands above the original SEU protein only in the reaction containing His-SUMO1^{GG} and SIZ1, but not in the other reactions (Figure 1E), suggesting that SEU is SUMOylated *in vitro* and its SUMOylation requires the presence of SUMO E3 ligase. Taken collectively, these results demonstrate that SEU is SUMOylated and is a bona fide substrate of SUMO1.

SIZ1 Interacts with SEU and Regulates Its SUMOylation

As SIZ1 is a key SUMO E3 ligase, we assessed whether SEU could interact with SIZ1 using a yeast two-hybrid assay. Because GBD-SIZ1 exhibited auto-activation activity that interfered with the assay, we used a truncated version, GBD-SIZ1-Δ (amino acids 1–664 of SIZ1 fused with the GAL4 DNA-binding domain). Indeed, GAD-SEU (SEU fused with the GAL4 activation domain) strongly interacted with GBD-SIZ1-Δ (Figure 2A). GAD-SEU also interacted with GBD-SCE1 (a SUMO-conjugating enzyme), but not GBD-SUMO1 (Figure 2A).

Next, we performed a semi-*in vitro* pull-down assay in *N. benthamiana* leaves, in which MBP-SEU-FLAG was incubated with SIZ1-Δ-FLAG. Precipitation with MBP beads revealed that SEU interacts with the truncated version of SIZ1 (Figure 2B). The *in vitro* pull-down assay of MBP-SEU-FLAG incubated with MBP-SIZ1-Myc demonstrates that SEU directly interacts with full-length SIZ1 (Figure 2C). *SEUp:SEU-GFP* fully complemented the short-hypocotyl phenotype of *seu-6* (see Figure 3A in detail; Huai et al., 2018). An *in vivo* co-immunoprecipitation (Co-IP) assay showed that the anti-GFP antibody immunoprecipitated SIZ1 from *seu-6/SEUp:SEU-GFP* plants, but not *seu-6* mutant plants

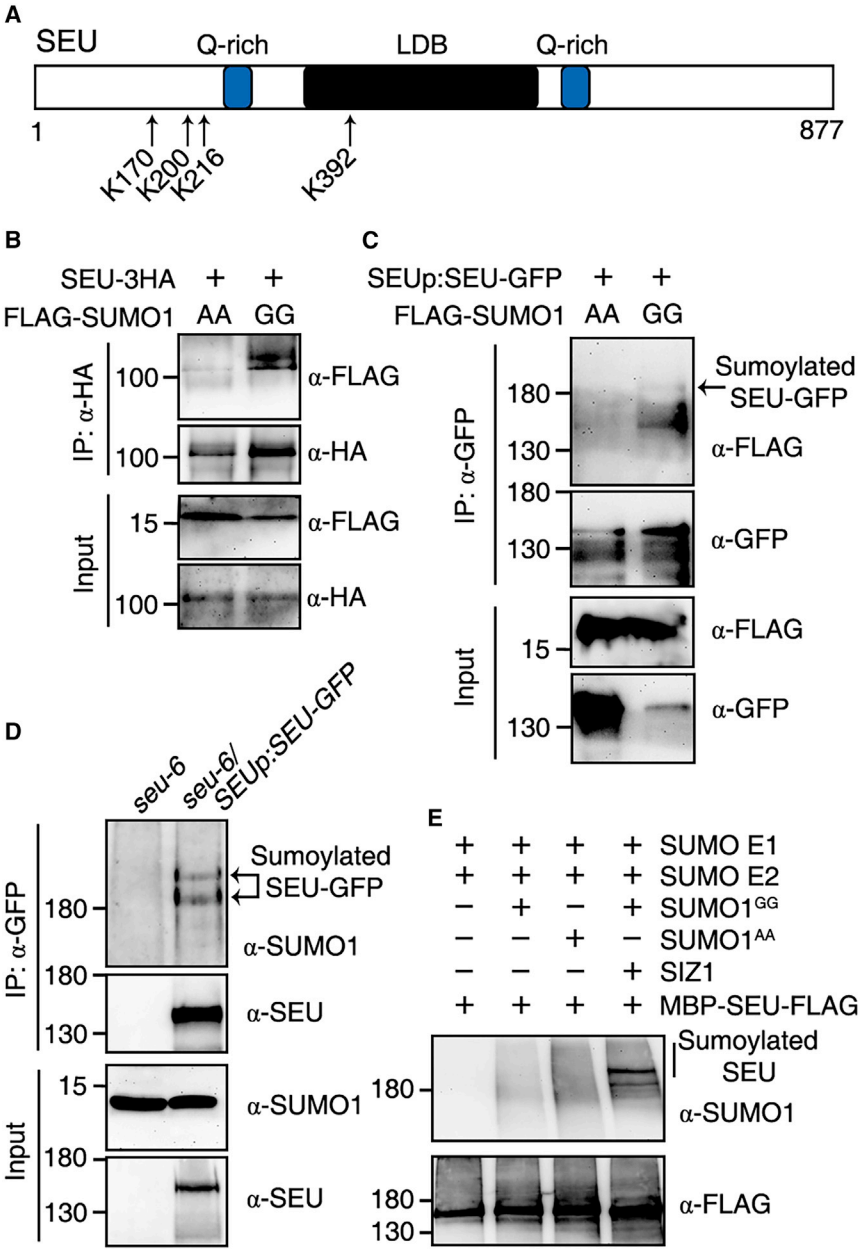

Figure 1. SEU Is Subject to SUMO Modification.

(A) Diagram of SEU structure and positions of four predicted SUMOylation sites. LDB, LIM-domain binding.

(B and C) Transient SUMOylation assay. FLAG-SUMO^{AA} or FLAG-SUMO^{GG} together with SEU-3HA **(B)** or SEUp:SEU-GFP **(C)** were transiently expressed in *Arabidopsis* protoplasts and *N. benthamiana* leaves, respectively. Total proteins were extracted and precipitated with an anti-HA or anti-GFP antibody and then immunoblotted with different antibodies.

(D) *In vivo* SUMOylation of SEU. Plants were grown under light (80 μmol/m^2/s) for 5 d. Proteins were precipitated with an anti-GFP monoclonal antibody conjugated to agarose beads.

(E) *In vitro* SUMOylation of SEU. SUMOylated MBP-SEU-FLAG was detected with an anti-SUMO1 antibody.

(Figure 2D). These results demonstrate that SEU interacts with SIZ1 *in vitro* and *in vivo*.

To investigate the functional relationship between SIZ1 and SEU, we generated a *seu siz1* double mutant. The hypocotyl length of *seu siz1* plants was slightly but significantly shorter than that of *seu* and *siz1* single mutants (Supplemental Figure 2A). *SEUp:SEU-GFP* largely complemented the *seu* phenotype, but this effect was partly suppressed in the *siz1* background (Supplemental Figure 2A). Similarly, at the adult stage, *seu siz1* plants showed a severe dwarf phenotype, much more extreme than the phenotypes of the parental single mutants. The complementary effect of *SEUp:SEU-GFP* on *seu-6* was largely inhibited by the *siz1* mutation (Supplemental Figure 2B and 2C). These observations suggest that SEU and SIZ1 coordinate plant growth and development, and that the function of SEU largely requires SIZ1. Furthermore, the *in vivo* immunoblotting experiment showed that the SUMOylated SEU-GFP bands seen in *seu-6/SEUp:SEU-GFP* were almost abolished in *siz1 seu-6/SEUp:SEU-GFP* (Figure 2E). Moreover, SEU protein levels were partially reduced in the *siz1* mutant in comparison with those in Col (Figure 2F), likely due to the transcriptional regulation by SIZ1 (Figure 2G). These results demonstrate that SIZ1 directly mediates the SUMOylation of SEU.

SUMOylation of SEU Is Required for Its Function

To investigate the functional importance of SEU SUMOylation, we substituted the four conserved K residues with arginine (R; non-SUMOylated form) via site-directed mutagenesis and

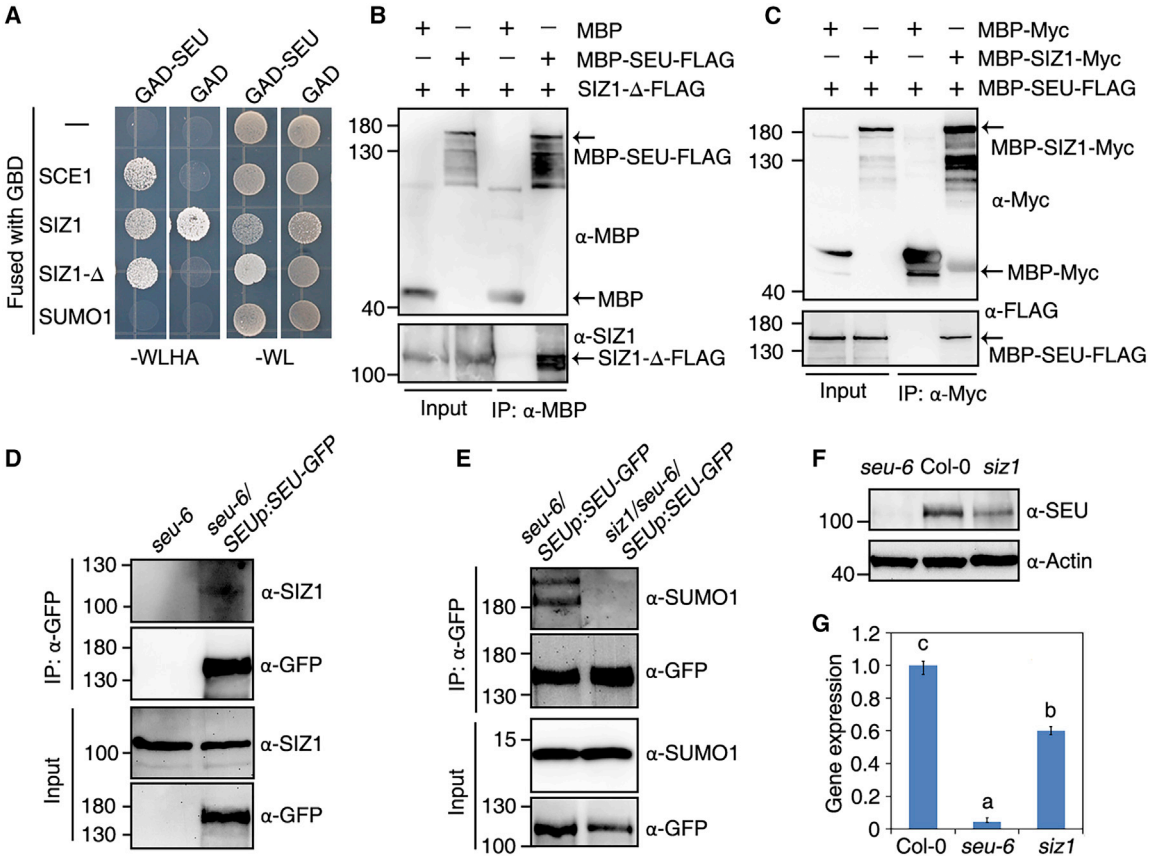

Figure 2. SIZ1 E3 Ligase Interacts with SEU and Regulates Its SUMOylation.

(A) Yeast two-hybrid assay. GAD, GAL4 activation domain; GBD, GAL4 DNA-binding domain; SIZ1-Δ, a truncated version of SIZ1 containing amino acids 1–664. −WLHA, without Trp, Leu, His, and Ade; −WL, without Trp and Leu.

(B) Semi-*in vitro* pull-down assay in *N. benthamiana* leaves.

(C) *In vitro* pull-down assay.

(D) Co-IP assay. Plants were grown under light (80 μmol/m^2/s) for 5 d. Proteins were precipitated with an anti-GFP antibody conjugated to agarose beads.

(E) Detection of SUMOylated proteins *in vivo*. Proteins were precipitated with an anti-GFP antibody conjugated to agarose beads.

(F) Immunoblot analysis of SEU. Blotting with an anti-actin antibody served as a loading control.

(G) qRT–PCR analysis of *SEU* expression. Relative gene expression was normalized to the level of *IPP2*. Data are means ± SD of three biological replicates. Different letters indicate significant differences as determined by one-way ANOVA ($P < 0.01$). In (**E**)–(**G**), seedlings were grown under red light (40 μmol/m^2/s) for 5 d.

generated transgenic lines expressing various forms of SEU fused with GFP (*SEUp:SEU(m)-GFP*: m stands for various K-to-R mutations) in the *seu-6* background. Multiple lines of transgenic plants expressing *SEUp:SEU(K170R)-GFP*, *SEUp:SEU(K200R)-GFP*, *SEUp:SEU(K216R)-GFP*, or *SEUp:SEU(K392R)-GFP* partly rescued the *seu-6* phenotype under red, far-red, and blue light conditions, with *SEUp:SEU(K392R)-GFP* having the weakest effect (Figure 3A, Supplemental Figure 3), suggesting that all four lysine (K) residues contribute to the function of SEU. Quadruple mutation of all four K sites in *SEUp:SEU(4KR)-GFP* resulted in phenotypes similar to those resulting from the single mutations (Figure 3A, Supplemental Figure 3). Consistent with this, the expression levels of two downstream genes, *INDOLE-3-ACETIC ACID INDUCIBLE6* (*IAA6*) and *IAA19*, in *seu-6/SEUp:-SEU(m)-GFP* plants were similar to those in *seu-6* plants (Figure 3B), suggesting that the SUMO modification of SEU affects its regulation of downstream genes. However, SEU protein levels of various mutant variants were comparable to that of wild-type SEU (Figure 3C).

Next, we examined the SUMOylation levels in these different transgenic mutant lines. SUMOylation expression in the K170R mutant was abolished, and its expression levels in K200R and K216R were largely reduced, whereas that in K392R was not altered compared with that in the wild type (Figure 3D). No SUMOylated band was detected in the 4KR mutant with K-to-R substitutions of all four K sites (Figure 3D). These results indicate that K170 is the major SUMOylation site. The K200R and K216R substitutions affected the efficiency of K170 SUMOylation, possibly by affecting the conformation of the region containing K170. Single or quadruple mutations did not affect nuclear localization (Supplemental Figure 4).

SEU is also involved in regulating thermomorphogenesis, and the *seu* mutant has reduced sensitivity to ambient warm temperature (Huai et al., 2018). *SEUp:SEU-GFP* completely restored the phenotype of the *seu-6* plants at 28°C. Interestingly, at this temperature, the hypocotyl length of *seu-6/SEUp:SEU(4KR)-GFP* was indistinguishable from that of *seu-6* (Figure 3E and

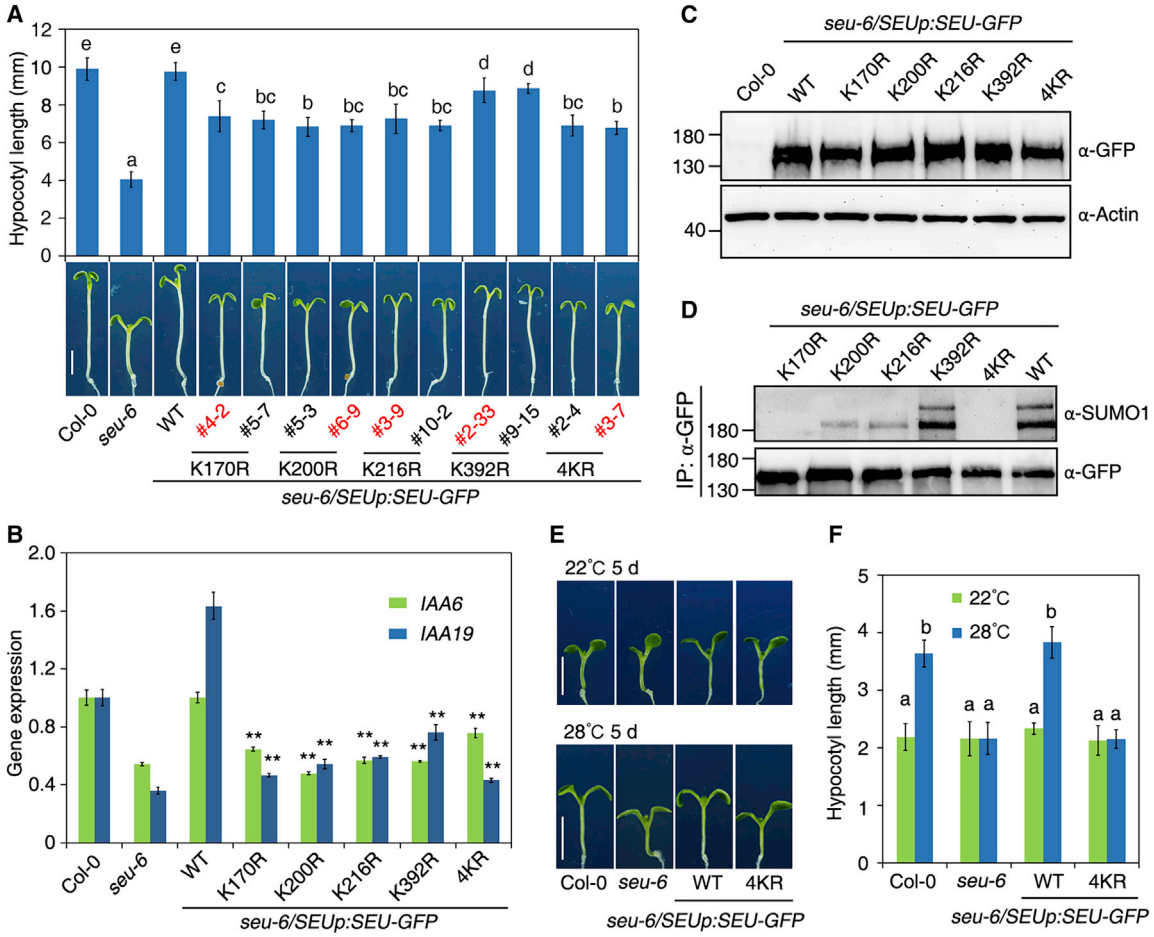

Figure 3. SUMOylation Is Required for the Function of SEU.

(A) Phenotype and hypocotyl length of Col, *seu-6*, and the indicated transgenic plants. Scale bar, 2 mm. Data are means ± SD of 20 seedlings. Different letters indicate significant differences as determined by one-way ANOVA ($P < 0.01$). Numbers shown in red denote the corresponding lines used in the following experiments.

(B) qRT–PCR analysis. Relative expression of *IAA6* and *IAA19* was normalized to the level of *IPP2*. Data are means ± SD of three biological replicates. Asterisks indicate significant differences from *seu-6/SEUp:SEU-GFP* (WT) using Student's *t*-test ($P < 0.01$).

(C) Immunoblotting assay. Blotting with an anti-actin antibody served as a loading control.

(D) SUMOylation assay. Proteins were precipitated with an anti-GFP antibody and then immunoblotted with an anti-SUMO1 or anti-GFP antibody. For (**A**)–(**D**), plants were grown under red light (40 μmol/m^2/s) for 5 d.

(E and F) Phenotype **(E)** and hypocotyl length **(F)** of plants grown at 22°C or 28°C for 5 d. Scale bars, 2 mm. Data are means ± SD of 20 seedlings. Different letters indicate significant differences as determined by one-way ANOVA ($P < 0.01$).

3F), which may be due to the increased SUMOylation at high temperature (Rytz et al., 2018).

K-to-R Substitution of SEU Affects Its Interaction with PIF4

SEU directly interacts with the PIF4 transcription factor and the two proteins coordinately regulate target gene expression (Huai et al., 2018). We therefore examined whether SUMOylation affects the SEU–PIF4 interaction. In a yeast two-hybrid assay, SEU^{4KR} fused with the GAL4 DNA-binding domain (GBD-SEU^{4KR}) interacted strongly with PIF4 or PIF4-C fused with the GAL4 activation domain (GAD-PIF4, GAD-PIF4C) in the presence of 3-amino-1,2,3-triazole inhibitor, whereas the GBD-SEU control showed almost no interaction (Figure 4A). These results suggest that these K-to-R point mutations in SEU affect its interaction with PIF4. In a Co-IP assay, a greater amount of PIF4 was pulled down in *seu-6/SEUp:SEU(4KR)-GFP* plants compared with *seu-6/SEUp:SEU-GFP* plants upon precipitation with an anti-GFP antibody (Figure 4B), implying that SEU SUMOylation might reduce its interaction with PIF4. To test whether the presence of SUMO1 can affect the interaction between SEU and PIF4, we assessed SUMO1's influence on the binding ability of SEU and PIF4 in a pull-down assay. MBP-SEU-FLAG and PIF4-GST were incubated with increasing amounts of His-SUMO1 and then pulled down with dextran Sepharose high performance (MBP beads). With increasing His-SUMO1, a decreasing amount of PIF4-GST was detected using an anti-GST antibody (Figure 4C). We excluded the possibility of SUMOylation due to the absence of necessary enzymes for SUMOylation. PIF4 has a SUMO-interaction domain in amino acids 27–31 based on site prediction with GPS-SUMO. It is likely that SUMO1 interacts with PIF4 and competes with SEU.

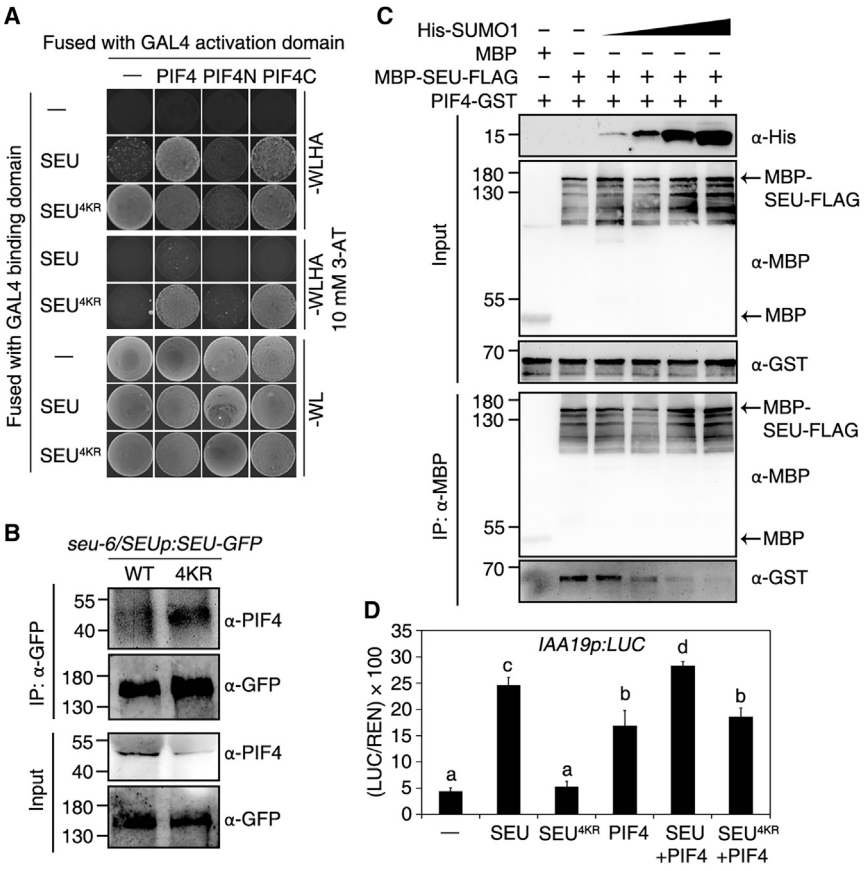

Figure 4. Mutations in the SUMOylation Sites of SEU Affect Its Interaction with PIF4.

(A) Yeast two-hybrid assay between SEU and PIF4. −WLHA, without Trp, Leu, His, and Ade; −WL, without Trp and Leu.

(B) Co-IP assay. Plants were grown under light (80 μmol/m^2/s) for 5 d. Proteins were precipitated with an anti-GFP antibody conjugated to agarose beads.

(C) His-SUMO1 inhibits the interaction of SEU and PIF4 in a pull-down assay. MBP-SEU-FLAG and PIF4-GST were incubated with increasing amounts of His-SUMO1 and precipitated with MBP beads.

(D) Transient expression assay of *IAA19p:LUC* in protoplasts. Relative LUC levels were expressed as the ratio of LUC luminescence normalized to REN luminescence (internal control). Data are means ± SD of three biological replicates. Different letters indicate significant differences as determined by one-way ANOVA ($P < 0.05$).

Next, we used the promoter of *IAA19*, a gene downstream of SEU in the photomorphogenesis pathway (Huai et al., 2018), to drive the luciferase reporter gene and then performed a transient luciferase reporter assay. Overexpression of either wild-type SEU or PIF4 activated *IAA19p:LUC* activity, and coexpression of SEU and PIF4 further increased this effect (Figure 4D). However, overexpression of SEU^{4KR} repressed *IAA19p:LUC* activity. Furthermore, the coexpression of SEU^{4KR} and PIF4 resulted in lower *IAA19p:LUC* activity than the coexpression of SEU and PIF4 (Figure 4D). Our previous study showed that SEU positively regulates the level of tri-methylation of lysine 4 of histone 3 (H3K4me3) at the chromatin region of *IAA19* (Huai et al., 2018). Consistently, the levels of H3K4me3 were reduced in the chromatin region containing the G-box of *IAA19* in *seu-6/SEUp:SEU(4KR)-GFP* compared with those in *seu-6/SEUp:SEU-GFP* (Supplemental Figure 5). These results imply that SEU SUMOylation promotes its transcriptional co-regulatory activity toward downstream gene expression.

SEU Physically Interacts with phyB

The phyB-PIF4 and SEU-PIF4 interaction prompted us to investigate whether SEU interacts with phyB directly. Firstly, we performed a semi-*in vitro* pull-down assay in which protein extracts from Col or *35S:Myc-phyB* plants were incubated with recombinant proteins (MBP or MBP-SEU-FLAG). The anti-Myc antibody pulled down MBP-SEU-FLAG when incubated with proteins from *35S:Myc-phyB*, but not from Col (Figure 5A). Secondly, we performed a luciferase complementation imaging assay and observed that the coexpression of SEU-nLUC (SEU fused with the N terminus of luciferase) and phyB-cLUC (phyB fused with the N terminus of LUC) generated luminescent signals in *N. benthamiana* leaves (Figure 5B). Thirdly, an *in vivo* Co-IP experiment showed that the anti-SEU antibody immunoprecipitated phyB from Col plants, but not from *seu* mutant plants (Figure 5C). Similarly, the anti-Myc antibody pulled down SEU from protein extracts of *35S:Myc-phyB*, but not of Col (Supplemental Figure 6A). Fourthly, a Co-IP assay further showed that SEU was pulled down by the anti-Myc antibody in *35S:Myc-phyB* seedlings (not in Col) grown under red light for 24 h, but not in the dark (Figure 5D). These results suggest that the Pfr form of phyB possibly associated with SEU more strongly than the Pr form. To test our speculation, total proteins of *35S:Myc-phyB* seedlings grown under red light for 5 d were exposed to 5 min of far-red light (for conversion to the Pr form), or 5 min of far-red light, followed immediately by 5 min of red light (for conversion back to the Pfr form). More SEU was immunoprecipitated by the anti-Myc antibody in *35S:Myc-phyB* seedlings under the far-red-to-red light transition than those under far-red light (Figure 5E). Therefore, we conclude that SEU interacts with the Pfr form of phyB.

Light Promotes SEU Protein Accumulation and SUMOylation

We then generated a *seu phyB* double mutant and found that the hypocotyl length of these plants was similar to that of the *phyB-9* single mutants (Figure 6A), indicating that the phenotype of the *seu* mutant is dependent on phyB. An immunoblot assay further showed that SEU protein accumulation was greatly reduced in

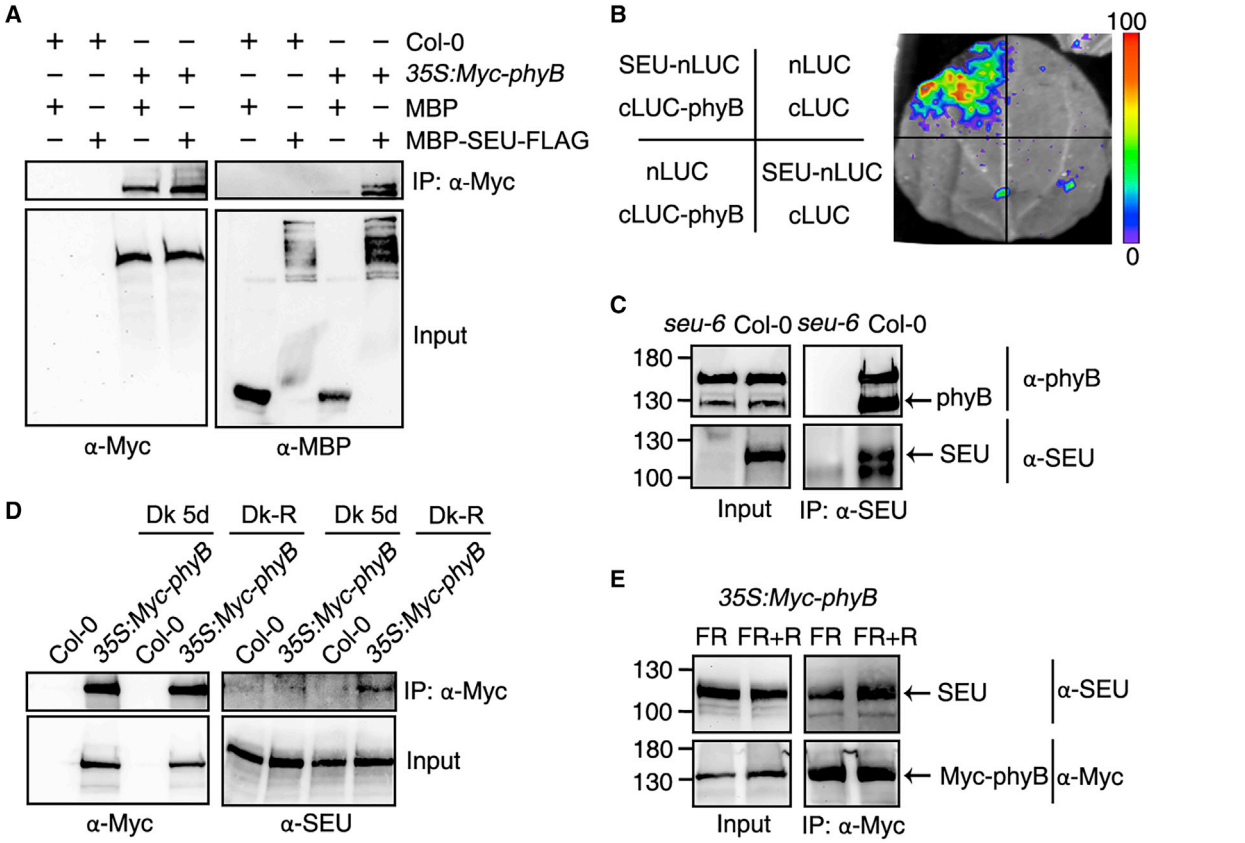

Figure 5. SEU Interacts with phyB.

(A) Semi-*in vitro* pull-down assay. Plants were grown under light (80 μmol/m^2/s) for 5 d. Plant proteins were extracted and incubated with MBP or MBP-SEU-FLAG recombinant proteins, and the mixtures were precipitated with an anti-Myc antibody.

(B) Split luciferase complementation imaging assay in *N. benthamiana*. nLUC, N terminus of LUC; cLUC, C terminus of LUC. After co-infiltration, plants were incubated for 3 d, and the luminescence intensity was determined.

(C) Co-IP assay. Plants were grown under light (80 μmol/m^2/s) for 5 d, and total proteins were immunoprecipitated with an anti-SEU antibody.

(D) Co-IP assay. Col and *35S:Myc-phyB* seedlings were grown in the dark (Dk) for 5 d or transferred to red light (R) (40 μmol/m^2/s) for 24 h. Total proteins were immunoprecipitated with an anti-Myc antibody.

(E) Co-IP assay. *35S:Myc-phyB* seedlings were grown under R (40 μmol/m^2/s) for 5 d. Total proteins were extracted and exposed to 5 min of far-red light (FR) (12 μmol/m^2/s) or followed by an additional 5 min of R light.

the *phyB-9* mutant compared with the wild type under red light (Figure 6B), whereas the *SEU* transcript level was not dramatically affected by the *phyB-9* mutation (Supplemental Figure 6B), suggesting that phyB positively regulates SEU protein accumulation.

Next, we investigated how light regulates SEU SUMOylation and its protein level. We compared the levels of SEU protein over time in *seu-6/SEUp:SEU-GFP* and *seu-6/SEUp:SEU(4KR)-GFP* seedlings grown under changing light conditions. During the dark-to-light transition, SEU protein levels were gradually increased in *seu-6/SEUp:SEU-GFP* seedlings, whereas they were almost unaffected in *seu-6/SEUp:SEU(4KR)-GFP* seedlings (Figure 6C and 6D). During the light-to-dark transition, SEU protein levels were gradually decreased in *seu-6/SEUp:SEU-GFP* seedlings, whereas they were almost unaffected in *seu-6/SEUp:SEU(4KR)-GFP* seedlings (Figure 6E and 6F). Furthermore, an *in vivo* immunoblotting assay showed that the SUMOylated SEU levels also gradually increased in *seu/SEUp:SEU-GFP* seedlings during the dark-to-light transition but decreased during the light-to-dark transition (Figure 6G and 6H). Taken collectively, these results indicate that light regulates SEU protein accumulation and SUMOylation. In addition, we tested the SUMOylation levels of SEU at different temperatures. An *in vivo* immunoblotting assay showed that SUMOylated SEU levels in *seu-6/SEUp:SEU-GFP* seedlings grown under 28°C were higher than those grown under 22°C (Supplemental Figure 7).

DISCUSSION

Compared with protein phosphorylation and ubiquitination, SUMO modification is less well understood in the field of plant photobiology. Previous studies have reported that phyB and COP1 are modified by SUMOylation (Sadanandom et al., 2015; Lin et al., 2016). In this study, we provide multiple lines of biochemical and genetic evidence that SEU is also regulated by SUMOylation. Firstly, a SUMOylation assay showed that SEU is a substrate of SUMO1 (Figure 1), consistent with a previous proteomic study (Miller et al., 2010). Secondly, we identified four conserved lysine residues corresponding to the

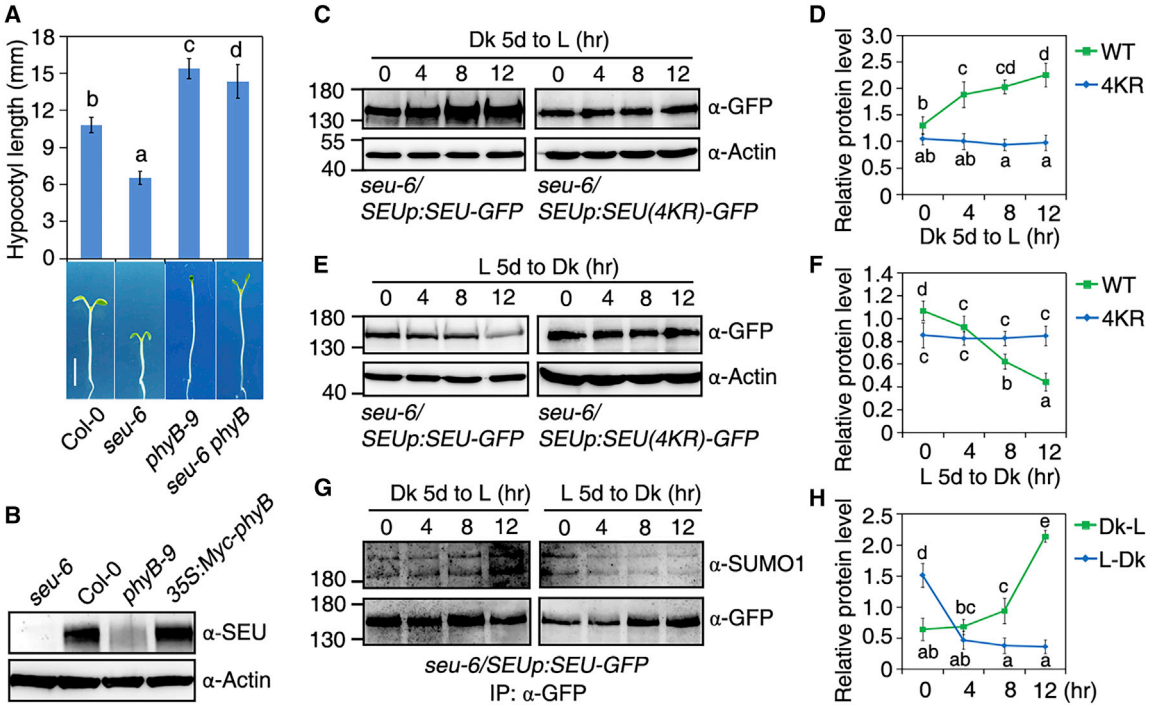

Figure 6. Light Regulates the Protein Accumulation and SUMOylation of SEU.

(A) Phenotype and hypocotyl length of seedlings grown under red light (40 μmol/m^2/s) for 5 d. Scale bar, 2 mm. Data are means ± SD of 20 plants. Different letters indicate significant differences as determined by one-way ANOVA ($P < 0.01$).

(B) Immunoblot analysis of SEU in plants grown under red light (40 μmol/m^2/s) for 5 d. Blotting with an anti-actin antibody served as a loading control.

(C) Immunoblot analysis. Seedlings were grown in the dark (Dk) for 5 d and transferred to white light (L) (80 μmol/m^2/s) for up to 12 h.

(D) Quantification of bands in **(C)**.

(E) Immunoblot analysis. Seedlings were grown in white light (80 μmol/m^2/s) for 5 d and transferred into darkness for up to 12 h. For (**C**) and (**E**), total proteins were immunoblotted with an anti-GFP antibody. Blotting with an anti-actin antibody served as a loading control.

(F) Quantification of bands in **(E)**.

(G) Detection of SUMOylated proteins in *seu-6/SEUp:SEU-GFP* plants during dark-to-light and light-to-dark transitions. Total proteins were precipitated with an anti-GFP antobody conjugated to agarose beads and then immunoblotted with anti-GFP and anti-SUMO1 antibodies.

(H) Quantification of the bands in **(G)**.

For **(D)**, **(F)**, and **(H)**, data are means ± SD of three biological replicates. Different letters indicate significant differences using one-way ANOVA ($P < 0.05$).

SUMOylation sites and found that mutations affecting these residues, especially K170R, K200R, and K216R, reduced or impaired SUMOylation, and altered SEU function (see discussion below). Thirdly, we showed that SIZ1, a key SUMO E3 ligase, interacts with SEU and controls its SUMOylation (Figure 2), confirming that SEU is subject to the SUMO modification. Consistently, SIZ1 was demonstrated to negatively regulate photomorphogenesis (Lin et al., 2016). Fourthly, we determined that light regulates SEU at the post-translational level, but not the transcriptional level (Figure 7; Huai et al., 2018).

SUMOylation represses or promotes the ubiquitination of its substrates, affecting protein subcellular localization, enzymatic activity, and protein–protein interactions (Geoffroy and Hay, 2009; Elrouby et al., 2013; Augustine and Vierstra, 2018). In this study, using site-directed mutagenesis and transgenic approaches, we revealed that residues K170, K200, and K216 were important for the function of SEU in photo- and thermomorphogenesis, whereas K392 played a weak role in these processes (Figure 3). The lysine-to-arginine substitutions of K200R and K216R each drastically reduced the SUMOylation level of SEU, and SUMOylation was almost undetectable in the K170R mutant, whereas it was unaffected in the K392R mutant (Figure 3C). The phenotype of the quadruple mutant carrying all four substitutions (4KR) was similar to those of K170, K200, and K216 single mutants. Thus, K170 is the predominant SUMOylation site. These mutations did not affect the protein levels or subcellular localization of SEU (Figure 3B, Supplemental Figure 4). However, the substitution of 4KR reduced the transcriptional activation activity of SEU toward *IAA19p:LUC* but enhanced its physical interaction with PIF4, and SUMO1 blocked the SEU-PIF4 interaction (Figure 4), indicating that SIZ1-mediated SUMOylation enhances the transcriptional activation activity of SEU but weakens its interaction with other factors. Notably, the mutations in the 4KR mutant partially complemented the photomorphogenic phenotype of the *seu* mutant, but fully restored its responsiveness to high temperature (Figure 3), suggesting that SEU regulates photo- and thermomorphogenesis in both overlapping and distinct ways. Interestingly, loss of *SIZ1* does not affect COP1 protein accumulation (Lin et al., 2016). SEU is possibly also subject to ubiquitination, and both SUMOylation and ubiquitination of SEU may involve the same lysine residue(s). Therefore, ubiquitin-

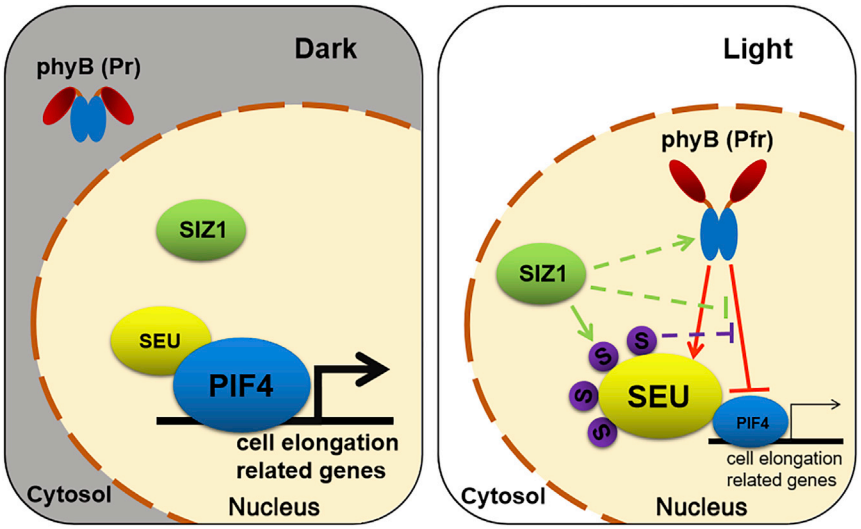

Figure 7. Proposed Working Model of How SEU SUMOylation Regulates Light Signaling.

In the darkness, SEU interacts with PIF4 to activate the expression of cell elongation-related genes (Huai et al., 2018). Red light triggers the activation of phyB (Pfr), which promotes SEU accumulation but PIF4 degradation. SIZ1-mediated SEU SUMOylation under light probably partially represses SEU-PIF4 interaction, thus further dampening the over-suppressive effect of PIF4 on photomorphogenesis. This may repress the degradation of PIF4. SIZ1 might also regulate phyB and PIF4. Arrows, activation; bars, repression. Dashed lines indicate indirect regulation (unknown mechanisms).

and proteasome-mediated degradation is likely inhibited by SUMOylation. Similarly, SIZ1 stabilizes MYB30 during ABA treatment and may also promote ICE1 stability (Miura et al., 2007; Zheng et al., 2012).

Intriguingly, our data demonstrate that SEU interacts with the phyB photoreceptors, and that this interaction is greatly enhanced under red light (Figure 5), suggesting that SEU may transduce phyB signals by preferentially associating with the active Pfr form of phyB. Consequently, phyB positively regulates the accumulation of SEU protein under red light (Figure 6B). Moreover, we showed that SEU accumulates during the dark-to-light transition but gradually degrades after the light-to-dark transition; however, the protein levels were not altered when the four SUMOylated residues were mutated (Figure 6), implying that light promotes SEU SUMOylation and stability. Similarly, red light enhances the accumulation of SUMOylated phyB (Sadanandom et al., 2015). SEU and PIF4 physically interact and co-regulate downstream gene expression (Huai et al., 2018). Upon light exposure, phyB interacts with PIF4 and triggers its degradation through the 26S proteasome pathway, thus relieving the inhibitory role of PIF4 on photomorphogenesis (Huq and Quail, 2002; Zhang et al., 2017a). Therefore, the stability of PIF4 and SEU are opposite in response to light, even though both proteins are negative regulators of photomorphogenesis. SEU might act to dampen the over-suppressive effect of PIF4 on photomorphogenesis, possibly by repressing the degradation of PIF4.

In summary, we propose that light activates phyB, which interacts with PIF4 and SEU, leading to the degradation of PIF4 but the stabilization of SEU. The SUMOylation of SEU promotes its transcriptional activation activity and reduces its interaction with PIF4, thus fine-tuning the transcription of PIF4 target genes and photomorphogenesis (and thermomorphogenesis) under changing light (and temperature) conditions (Figure 7). PIF4 might also be modulated by SUMOylation (Mazur et al., 2019). The SUMO modification precisely regulates the activity of these proteins and modulates their stability and interaction with other factors. Sequence analysis revealed that the SUMOylated lysine residues in SEU are conserved in various plant species, implying that the SUMO regulation and function of SEU might be conserved during evolution in land plants.

MATERIALS AND METHODS

Plant Materials

The *seu-6* (Huai et al., 2018), *phyB-9* (Zhang et al., 2017c), and *siz1* (Salk_065397) (Niu et al., 2019) mutants were in the Columbia (Col-0) ecotype background. The *seu siz1*, *seu phyB*, and *siz1 seu-6/pSEU:SEU(4KR)-GFP* mutants were generated by genetic crossing. All homozygous mutant and transgenic lines were verified by PCR genotyping and/or antibiotic selection. Primers are listed in Supplemental Table 1. Transgenic plants were generated by *Agrobacterium tumefaciens*-mediated transformation via the floral dip method (Clough and Bent, 1998) and selected on MS plates in the presence of antibiotics. Homozygous lines were used in the experiments.

Plant Growth Conditions and Phenotypic Analysis

Seeds were sown on 1× Murashige and Skoog medium containing 1% sucrose and 0.8% agar and incubated at 4°C in the dark for 3 d. For photomorphogenic experiments, seedlings were grown in the dark or under continuous far-red (12 μmol/m^2/s), red (40 μmol/m^2/s), or blue (10 μmol/m^2/s) light at 22°C for 5 d. For thermomorphogenic experiments, seedlings were grown under continuous white light (50 μmol/m^2/s) at 22°C or 28°C for 5 d. Light was supplied by light-emitting diodes. Representative seedlings were placed on agar plates and photographed with a digital camera (Olympus). Hypocotyl length was measured and analyzed using NIH ImageJ software (http://rsbweb.nih.gov/ij/).

Plasmid Construction

The coding sequences of *SEU*, *PIF4*, *SIZ1*, *SIZ1-Δ* (1–1993 bp), and the promoter of *IAA19* were amplified using high-fidelity *Pfu* DNA polymerase (Invitrogen) and cloned into the pEASY-Blunt vector (TransGen) to generate pEASY-SEU, pEASY-PIF4, pEASY-SIZ1, pEASY-SIZ1-Δ, and pEASY-IAA19p, respectively. The SUMOylation sites of lysine (K) in SEU were mutated to arginine (R) using the Fast Mutagenesis System kit (TransGen) to generate pEASY-SEU^{KR}. PCR primers are listed in Supplemental Table 1.

SEU was digested from pEASY-SEU and cloned into the pGADT7 vector (Clontech) to generate pGAD-SEU. *SEU*, *SEU^{KR}*, *SIZ1*, and *SIZ1-Δ* were digested from corresponding vectors and cloned into the pGBKT7 vector (Clontech) to generate pGBK-SEU, pGBK-SEU^{KR}, pGBK-SIZ1, and pGBK-SIZ1-Δ. *SEU*, *SEU^{KR}*, and *PIF4* were digested from corresponding pEASY vectors and cloned into the pUC18-3HA vector to generate SEU-3HA, SEU^{KR}-3HA, and PIF4-3HA. *IAA19p* was digested from pEASY-IAA19p and ligated into the pGREEN2-0800-LUC vector to generate *IAA19p:LUC.* *SEU* was digested from pEASY and inserted into pCAMBIA-1300-nLUC to generate SEU-nLUC. *SIZ1-Δ* was inserted into pCAMBIAKaBar-nFLAG to generate SIZ1-Δ-FLAG. pGAD-phyB and cLUC-phyB plasmids were generated by homologous recombination. pGAD-PIF4, pGAD-PIF4-N, pGAD-PIF4-C, and MBP-SEU-FLAG were produced as described previously (Huai et al., 2018).

SEU^{KR} fragments were digested from the corresponding pEASY vectors and cloned into SEUp:GFP (Huai et al., 2018) to generate the SEUp:SEU^{KR}-GFP binary vector. The binary vectors were electroporated into the *Agrobacterium tumefaciens* strain GV3101 and introduced into *Arabidopsis* via the floral dip method (Clough and Bent, 1998). Transgenic plants were selected on MS plates in the presence of hygromycin. Homozygous lines were used in the experiments.

SUMOylation Site Prediction

Putative SUMOylation sites in SEU were identified using GPS-SUMO (http://sumosp.biocuckoo.org/online.php), the SUMOplot Analysis Program (Abgent) (http://www.abgent.com/sumoplot), and JASSA (http://www.jassa.fr/index.php?m=jassa). The conservation of the predicted SUMOylation sites and SUMO-binding motifs of SEU between *Arabidopsis*, *Oryza sativa*, *Zea mays*, *Helianthus annuus*, and *Populus trichocarpa* were analyzed using DNAMAN software.

qRT–PCR

Total RNA was extracted from seedlings or rosette leaves using the RNA Prep Pure Plant kit (Tiangen), and cDNA was synthesized using reverse transcriptase (Invitrogen). Quantitative PCR was performed using the SYBR Premix ExTaq kit (Takara) in a LightCycler 480 (Roche) according to the manufacturer's instructions. Three biological replicates were performed, and the relative expression level of each gene was normalized to that of *ISOPENTENYL PYROPHOSPHATE: DIMETHYLALLYL PYROPHOSPHATE ISOMERASE* (*IPP2*, control). PCR primers are listed in Supplemental Table 1. Each experiment was repeated at least three times.

Yeast Two-Hybrid Assay

The bait construct fused with GBD and the prey construct fused with GAD were co-transformed into the yeast Y2HGold strain (Clontech). Transformants were grown on synthetic dropout (SD)-Trp/Leu and SD-Trp/Leu/His/Ade selective medium with or without 3-amino-1,2,4-triazole and incubated at 30°C for 2–6 d.

Immunoblot Analysis

Total proteins were extracted with extraction buffer (50 mM Tris–HCl [pH 7.5], 150 mM NaCl, 10 mM $MgCl_2$, 0.1% Tween 20, 1 mM phenylmethylsulfonyl fluoride, and 1× complete protease inhibitor cocktail [Roche, 04693159001]) and quantified using the Bradford assay (Bio-Rad). Samples were boiled at 95°C for 5 min in 2× SDS loading buffer and separated on SDS–PAGE gels. Proteins were transferred to polyvinylidene difluoride membranes and immunoblotted with an anti-SEU (Huai et al., 2018) or anti-GFP antibody (TransGen, HT801), with an anti-actin antibody (CWBIO, CW0264M) as a loading control, and then immunoblotted with horseradish peroxidase-conjugated goat anti-rabbit IgG (CWBIO, CW0103S) or goat anti-mouse IgG (CWBIO, CW0102S). Signals were captured with a chemiluminescence imaging system (Biostep).

Co-IP Assay

Co-IP assays were performed as described previously (Lin et al., 2016) to detect protein–protein interactions. Total proteins were extracted from seedlings with extraction buffer containing 50 mM Tris–HCl (pH 7.4), 150 mM NaCl, 1 mM EDTA (pH 8.0), 1 mM DTT, 0.1% TritonX-100, and 1× complete protease inhibitor cocktail (Roche, 04693159001). Proteins were immunoprecipitated with antibody-conjugated agarose beads (20 μl) at 4°C for 2 h. Beads were washed three times with protein extraction buffer and eluted with 2× SDS loading buffer at 95°C for 5 min. Eluted proteins were detected by immunoblotting and analyzed with an anti-PIF4 (Huai et al., 2018), anti-phyB (Zhang et al., 2018), anti-SEU (Huai et al., 2018), anti-SIZ1 (Niu et al., 2019), anti-GFP, or anti-Myc antibody (TransGen, HT101).

Semi-*In Vitro* Pull-Down and Pull-Down Assays

MBP-, GST-, and His-fusion recombinant proteins were expressed and induced by isopropyl-beta-D-thiogalactopyranoside in the *Escherichia coli* BL21 (DE3) strain. Proteins were purified with dextran Sepharose high-performance beads (GE Healthcare, for MBP-fusion proteins), glutathione Sepharose 4B beads (GE Healthcare, for GST-fusion proteins), or Ni-NTA agarose (QIAGEN, for His-fusion proteins), respectively. Semi-*in vitro* pull-down and pull-down assays were performed as described previously (Jing et al., 2013; Yang et al., 2017). Aliquots of different purified fusion proteins were incubated at 4°C for 2 h. Beads (20 μl) were added to the samples, followed by gentle rotation at 4°C for 2 h. Input and IP proteins were detected with an anti-Myc, anti-FLAG (Sigma, F3165), anti-MBP (Abcam, ab9084), anti-GST (Abcam, ab19256), or anti-His antibody (Abcam, ab14923).

In Vivo SUMOylation Assay

To determine the SUMOylation status of SEU, proteins were extracted with SUMOylation buffer (50 mM Tris–Cl [pH 7.4], 150 mM NaCl, 1 mM EDTA [pH 8.0], 1 mM DTT, 20 mM N-ethylmaleimide [NEM, Sigma], 0.1% TritonX-100, and 1× complete protease inhibitor mixture [Roche, 04693159001]). The protein extracts were immunoprecipitated with 20 μl anti-GFP-conjugated agarose beads (MBL, D153-8) at 4°C for 2 h. The beads were washed three times with protein extraction buffer and eluted with 2× SDS loading for immunoblot analysis. The SUMOylated form of SEU was determined with an anti-SUMO1 antibody (Niu et al., 2019). Blotting with an anti-SEU or anti-GFP antibody was used as loading controls.

In Vitro SUMOylation Assay

The *in vitro* SUMOylation of SEU was examined as described previously (Lin et al., 2016). In brief, purified His-SUMO E1, His-SUMO E2, His-SUMO1, MBP-SIZ1-Myc, and MBP-SEU-FLAG recombinant proteins were purified. Proteins were then incubated in 30 μl of reaction buffer (20 mM HEPES [pH 7.5], 5 mM $MgCl_2$ and 2 mM ATP) at 30°C for 3 h. SUMOylated MBP-SEU-FLAG was detected with anti-FLAG (Sigma, F3165) and anti-SUMO1 antibodies.

Luciferase Complementation Imaging Assay

The *Agrobacterium tumefaciens* GV3101 strain (OD_{600} = 0.8) carrying SEU-nLUC and cLUC-phyB plasmids were co-infiltrated into young *N. benthamiana* leaves using a needleless syringe. *N. benthamiana* was exposed to weak light for 2 d. Thereafter, 1 mM luciferase substrate solution was sprayed onto *N. benthamiana* leaves, and the fluorescence intensity was recorded using bioluminescence *in vivo* imaging and analysis system (NightSHADE LB985, Berthold Technologies).

Transient Luciferase Reporter Assays

Five micrograms of the *IAA19p:LUC* reporter plasmid containing a REN expression cassette was co-transformed with 5 μg of SEU-3HA, SEU^{4KR}-3HA, PIF4-3HA, SEU-3HA and PIF4-3HA, or SEU^{4KR}-3HA and PIF4-3HA effector plasmids into *Arabidopsis* protoplasts. After overnight incubation in the dark, protoplasts were lysed and resuspended with lysis

reagent (Promega). The activities of firefly (*Photinus pyralis*) and *Renilla* (*Renilla reniformis*) luciferases (LUC and REN, respectively) were measured with a Modulus luminometer/fluorometer (Promega). REN was used as a control to monitor the transformation efficiency. Relative LUC levels were expressed as the ratio of LUC/REN.

GFP Fluorescence

seu-6/SEUp:SEU-GFP and *seu-6/SEUp:SEU(m)-GFP* transgenic seedlings were grown under white light for 5 d, and fluorescence was observed with a confocal microscope (Zeiss LSM 510). All images were captured using identical settings.

ChIP–qPCR Assay

Chromatin immunoprecipitation, followed by quantitative PCR, was performed as described previously (Huai et al., 2018).

SUPPLEMENTAL INFORMATION

Supplemental Information is available at *Plant Communications Online*.

FUNDING

This work was supported by grants from the National Key Research and Development Program of China (2016YFD0100405; 2017YFA0503800), the Strategic Priority Research Program of the Chinese Academy of Sciences (XDB27030205), and the National Natural Science Foundation of China (31800235).

AUTHOR CONTRIBUTIONS

X.Z. performed most of the experiments. J.H. constructed partial plant materials and performed ChIP and GFP fluorescence assays. S.L. generated the phyB constructs. J.J. discussed the paper and provided comments. All authors analyzed the data. X.Z. and R.L. designed the experiments and wrote the paper.

ACKNOWLEDGMENTS

We thank Dr. Jigang Li (China Agricultural University) for providing the anti-phyB antibody. No conflicts of interest are declared.

Received: November 23, 2019
Revised: May 25, 2020
Accepted: May 29, 2020
Published: June 2, 2020

REFERENCES

Augustine, R.C., and Vierstra, R.D. (2018). SUMOylation: re-wiring the plant nucleus during stress and development. Curr. Opin. Plant Biol. **45**:143–154.

Cai, B., Kong, X., Zhong, C., Sun, S., Zhou, X.F., Jin, Y.H., Wang, Y., Li, X., Zhu, Z., and Jin, J.B. (2017). SUMO E3 ligases GmSIZ1a and GmSIZ1b regulate vegetative growth in soybean. J. Integr. Plant Biol. **59**:2–14.

Clough, S.J., and Bent, A.F. (1998). Floral dip: a simplified method for *Agrobacterium*-mediated transformation of *Arabidopsis thaliana*. Plant J. **16**:735–743.

Conti, L., Nelis, S., Zhang, C., Woodcock, A., Swarup, R., Galbiati, M., Tonelli, C., Napier, R., Hedden, P., Bennett, M., et al. (2014). Small ubiquitin-like modifier protein SUMO enables plants to control growth independently of the phytohormone gibberellin. Dev. Cell **28**:102–110.

Crozet, P., Margalha, L., Butowt, R., Fernandes, N., Elias, C.A., Orosa, B., Tomanov, K., Teige, M., Bachmair, A., Sadanandom, A., et al. (2016). SUMOylation represses SnRK1 signaling in *Arabidopsis*. Plant J. **85**:120–133.

Elrouby, N., and Coupland, G. (2010). Proteome-wide screens for small ubiquitin-like modifier (SUMO) substrates identify *Arabidopsis* proteins implicated in diverse biological processes. Proc. Natl. Acad. Sci. U S A **107**:17415–17420.

Elrouby, N., Bonequi, M.V., Porri, A., and Coupland, G. (2013). Identification of *Arabidopsis* SUMO-interacting proteins that regulate chromatin activity and developmental transitions. Proc. Natl. Acad. Sci. U S A **110**:19956–19961.

Franks, R.G., Wang, C., Levin, J.Z., and Liu, Z. (2002). SEUSS, a member of a novel family of plant regulatory proteins, represses floral homeotic gene expression with LEUNIG. Development **129**:253–263.

Geoffroy, M.C., and Hay, R.T. (2009). An additional role for SUMO in ubiquitin-mediated proteolysis. Nat. Rev. Mol. Cell Biol. **10**:564–568.

Gommers, C.M., and Monte, E. (2018). Seedling establishment: a dimmer switch-regulated process between dark and light signaling. Plant Physiol. **176**:1061–1074.

Gong, X., Flores-Vergara, M.A., Hong, J.H., Chu, H., Lim, J., Franks, R.G., Liu, Z., and Xu, J. (2016). SEUSS integrates gibberellin signaling with transcriptional inputs from the SHR-SCR-SCL3 module to regulate middle cortex formation in the *Arabidopsis* root. Plant Physiol. **170**:1675–1683.

Grigorova, B., Mara, C., Hollender, C., Sijacic, P., Chen, X., and Liu, Z. (2011). LEUNIG and SEUSS co-repressors regulate *miR172* expression in *Arabidopsis* flowers. Development **138**:2451–2456.

Hoecker, U. (2005). Regulated proteolysis in light signaling. Curr. Opin. Plant Biol. **8**:469–476.

Huai, J., Zhang, X., Li, J., Ma, T., Zha, P., Jing, Y., and Lin, R. (2018). SEUSS and PIF4 coordinately regulate light and temperature signaling pathways to control plant growth. Mol. Plant **11**:928–942.

Huq, E., and Quail, P.H. (2002). PIF4, a phytochrome-interacting bHLH factor, functions as a negative regulator of phytochrome B signaling in *Arabidopsis*. EMBO J. **21**:2441–2450.

Jiao, Y., Lau, O.S., and Deng, X.W. (2007). Light-regulated transcriptional networks in higher plants. Nat. Rev. Genet. **8**:217–230.

Jin, J.B., Jin, Y.H., Lee, J., Miura, K., Yoo, C.Y., Kim, W.Y., Van Oosten, M., Hyun, Y., Somers, D.E., Lee, I., et al. (2008). The SUMO E3 ligase, AtSIZ1, regulates flowering by controlling a salicylic acid-mediated floral promotion pathway and through affects on *FLC* chromatin structure. Plant J. **53**:530–540.

Jing, Y., Zhang, D., Wang, X., Tang, W., Wang, W., Huai, J., Xu, G., Chen, D., Li, Y., and Lin, R. (2013). *Arabidopsis* chromatin remodeling factor PICKLE interacts with transcription factor HY5 to regulate hypocotyl cell elongation. Plant Cell **25**:242–256.

Johnson, E.S. (2004). Protein modification by SUMO. Annu. Rev. Biochem. **73**:355–382.

Jurata, L.W., and Gill, G.N. (1997). Functional analysis of the nuclear LIM domain interactor NLI. Mol. Cell. Biol. **17**:5688–5698.

Kim, S.I., Park, B.S., Kim, D.Y., Yeu, S.Y., Song, S.I., Song, J.T., and Seo, H.S. (2015). E3 SUMO ligase AtSIZ1 positively regulates SLY1-mediated GA signalling and plant development. Biochem. J. **469**:299–314.

Leivar, P., and Monte, E. (2014). PIFs: systems integrators in plant development. Plant Cell **26**:56–78.

Leivar, P., Monte, E., Oka, Y., Liu, T., Carle, C., Castillon, A., Huq, E., and Quail, P.H. (2008). Multiple phytochrome-interacting bHLH transcription factors repress premature seedling photomorphogenesis in darkness. Curr. Biol. **18**:1815–1823.

Leivar, P., Tepperman, J.M., Monte, E., Calderon, R.H., Liu, T.L., and Quail, P.H. (2009). Definition of early transcriptional circuitry involved in light-induced reversal of PIF-imposed repression of photomorphogenesis in young *Arabidopsis* seedlings. Plant Cell **21**:3535–3553.

Lin, X.L., Niu, D., Hu, Z.L., Kim, D.H., Jin, Y.H., Cai, B., Liu, P., Miura, K., Yun, D.J., Kim, W.Y., et al. (2016). An *Arabidopsis* SUMO E3 ligase, SIZ1, negatively regulates photomorphogenesis by promoting COP1 activity. PLoS Genet. **12**:e1006016.

Mazur, M.J., Kwaaitaal, M., Mateos, M.A., Maio, F., Kini, R.K., Prins, M., and van den Burg, H.A. (2019). The SUMO conjugation complex self-assembles into nuclear bodies independent of SIZ1 and COP1. Plant Physiol. **179**:168–183.

Miller, M.J., Barrett-Wilt, G.A., Hua, Z., and Vierstra, R.D. (2010). Proteomic analyses identify a diverse array of nuclear processes affected by small ubiquitin-like modifier conjugation in *Arabidopsis*. Proc. Natl. Acad. Sci. U S A **107**:16512–16517.

Miura, K., Rus, A., Sharkhuu, A., Yokoi, S., Karthikeyan, A.S., Raghothama, K.G., Baek, D., Koo, Y.D., Jin, J.B., Bressan, R.A., et al. (2005). The *Arabidopsis* SUMO E3 ligase SIZ1 controls phosphate deficiency responses. Proc. Natl. Acad. Sci. U S A **102**:7760–7765.

Miura, K., Jin, J.B., Lee, J., Yoo, C.Y., Stirm, V., Miura, T., Ashworth, E.N., Bressan, R.A., Yun, D.J., and Hasegawa, P.M. (2007). SIZ1-mediated sumoylation of ICE1 controls CBF3/DREB1A expression and freezing tolerance in *Arabidopsis*. Plant Cell **19**:1403–1414.

Miura, K., Lee, J., Jin, J.B., Yoo, C.Y., Miura, T., and Hasegawa, P.M. (2009). Sumoylation of ABI5 by the *Arabidopsis* SUMO E3 ligase SIZ1 negatively regulates abscisic acid signaling. Proc. Natl. Acad. Sci. U S A **106**:5418–5423.

Ni, W., Xu, S.L., Tepperman, J.M., Stanley, D.J., Maltby, D.A., Gross, J.D., Burlingame, A.L., Wang, Z.Y., and Quail, P.H. (2014). A mutually assured destruction mechanism attenuates light signaling in *Arabidopsis*. Science **344**:1160–1164.

Niu, D., Lin, X.L., Kong, X., Qu, G.P., Cai, B., Lee, J., and Jin, J.B. (2019). SIZ1-Mediated SUMOylation of TPR1 suppresses plant immunity in *Arabidopsis*. Mol. Plant **12**:215–228.

Orosa, B., Yates, G., Verma, V., Srivastava, A.K., Srivastava, M., Campanaro, A., De Vega, D., Fernandes, A., Zhang, C., Lee, J., et al. (2018). SUMO conjugation to the pattern recognition receptor FLS2 triggers intracellular signalling in plant innate immunity. Nat. Commun. **9**:5185.

Park, B.S., Song, J.T., and Seo, H.S. (2011). *Arabidopsis* nitrate reductase activity is stimulated by the E3 SUMO ligase AtSIZ1. Nat. Commun. **2**:400.

Pfeiffer, A., Shi, H., Tepperman, J.M., Zhang, Y., and Quail, P.H. (2014). Combinatorial complexity in a transcriptionally centered signaling hub in *Arabidopsis*. Mol. Plant **7**:1598–1618.

Rytz, T.C., Miller, M.J., McLoughlin, F., Augustine, R.C., Marshall, R.S., Juan, Y.T., Charng, Y.Y., Scalf, M., Smith, L.M., and Vierstra, R.D. (2018). SUMOylome profiling reveals a diverse array of nuclear targets modified by the SUMO ligase SIZ1 during heat stress. Plant Cell **30**:1077–1099.

Sadanandom, A., Ádám, É., Orosa, B., Viczián, A., Klose, C., Zhang, C., Josse, E.M., Kozma-Bognár, L., and Nagy, F. (2015). SUMOylation of phytochrome-B negatively regulates light-induced signaling in *Arabidopsis thaliana*. Proc. Natl. Acad. Sci. U S A **112**:11108–11113.

Seeler, J.S., and Dejean, A. (2003). Nuclear and unclear functions of SUMO. Nat. Rev. Mol. Cell Biol. **4**:690–699.

Shin, J., Kim, K., Kang, H., Zulfugarov, I.S., Bae, G., Lee, C.H., Lee, D., and Choi, G. (2009). Phytochromes promote seedling light responses by inhibiting four negatively-acting phytochrome-interacting factors. Proc. Natl. Acad. Sci. U S A **106**:7660–7665.

Sridhar, V.V., Surendrarao, A., and Liu, Z. (2006). APETALA1 and SEPALLATA3 interact with SEUSS to mediate transcription repression during flower development. Development **133**:3159–3166.

Yang, M., Li, C., Cai, Z., Hu, Y., Nolan, T., Yu, F., Yin, Y., Xie, Q., Tang, G., and Wang, X. (2017). SINAT E3 ligases control the light-mediated stability of the brassinosteroid-activated transcription factor BES1 in *Arabidopsis*. Dev. Cell **41**:47–58.

Zhang, B., Holmlund, M., Lorrain, S., Norberg, M., Bako, L., Fankhauser, C., and Nilsson, O. (2017a). BLADE-ON-PETIOLE proteins act in an E3 ubiquitin ligase complex to regulate PHYTOCHROME INTERACTING FACTOR 4 abundance. eLife **6**:e26759.

Zhang, S., Zhuang, K., Wang, S., Lv, J., Ma, N., and Meng, Q. (2017b). A novel tomato SUMO E3 ligase, SlSIZ1, confers drought tolerance in transgenic tobacco. J. Integr. Plant Biol. **59**:102–117.

Zhang, X., Huai, J., Shang, F., Xu, G., Tang, W., Jing, Y., and Lin, R. (2017c). A PIF1/PIF3-HY5-BBX23 transcription factor cascade affects photomorphogenesis. Plant Physiol. **174**:2487–2500.

Zhang, S., Li, C., Zhou, Y., Wang, X., Li, H., Feng, Z., Chen, H., Qin, G., Jin, D., Terzaghi, W., et al. (2018). TANDEM ZINC-FINGER/PLUS3 is a key component of phytochrome A signaling. Plant Cell **30**:835–852.

Zheng, Y., Schumaker, K.S., and Guo, Y. (2012). Sumoylation of transcription factor MYB30 by the small ubiquitin-like modifier E3 ligase SIZ1 mediates abscisic acid response in *Arabidopsis thaliana*. Proc. Natl. Acad. Sci. U S A **109**:12822–12827.